

DOI: 10.1515/amm-2016-0168

M. GWOŹDZIK\*\*

## THE DEFECTS OF OXIDE LAYERS FORMED ON 10CrMo9-10 STEEL OPERATED FOR 200,000 HOURS AT AN ELEVATED TEMPERATURE

The paper contains results of studies into the formation of oxide layers on 10CrMo9-10 (10H2M) steel long-term operated at an elevated temperature ( $T = 545^{\circ}\text{C}$ ,  $t = 200,000\text{h}$ ). The oxide layer was studied on a surface and a cross-section at the inner and outer surface of the tube wall on the outlet both on the fire and counter-fire side of the tube wall surface.

The obtained results of research have shown a higher degree of degradation, both of the steel itself and oxide layers, on the fire side. In addition, it has been shown that on the outside tube wall, apart from iron oxides, there are also deposits composed mainly of  $\text{Al}_2\text{SiO}_5$ .

*Keywords:* oxide layer, 10CrMo9-10 steel, LM, SEM, AFM, XRD

### 1. Introduction

Both low- and high-alloy steels are used in the power industry; they should ensure a safe operation of the equipment at an elevated temperature during a long time [1,2]. More and more research is carried out now on the corrosion resistance of 10CrMo9-10 steel operating at an elevated temperature [3-7].

Lehmusto et al. [3] studied inter alia the influence of KCl and  $\text{K}_2\text{CO}_3$  on 10CrMo9-10 steel oxidation at temperatures of 500, 550 and  $600^{\circ}\text{C}$  in short-term laboratory tests (168 h). They have shown that oxides forming on 10CrMo9-10 steel are iron oxides, which in the vicinity of steel are additionally enriched with chromium. It has been shown in that paper that the forming oxides layer depends not only on temperature and atmosphere but also on potassium compounds. The oxides formed in the presence of potassium carbonate are well-adhered, whereas the oxides formed in the presence of potassium chloride are multilayered, with poorly adhering layers.

Klepacki and Wywrot [8] have presented corrosion examples both on the steam flow side (inside) and on the flue gas side (outside). Such oxides as hematite ( $\text{Fe}_2\text{O}_3$ ) and magnetite ( $\text{Fe}_3\text{O}_4$ ) are formed on the inside tube wall, while on the flue gas side such alkaline-sulphate compounds are formed, as:  $\text{Na}_3\text{Fe}(\text{SO}_4)_3$  and  $\text{K}_3\text{Fe}(\text{SO}_4)_3$  as well as sulphate compounds like  $\text{FeSO}_4$ .

### 2. Material and experimental methods

The material studied comprised specimens of 10CrMo9-10 (10H2M) steel taken from a pipeline operated at the temperature of  $545^{\circ}\text{C}$  during 200,000 hours. The oxide layer was studied on a surface and a cross-section at the inner and outer surface of the tube wall on the outlet both on the fire and counter-fire side of the tube wall surface.

Thorough examinations of the oxide layer carried out on the inner and outer surface and fire wall and opposite fire wall of tube wall comprised:

- microscopic examinations of the oxide layer were performed using an Olympus GX41 optical microscope,
- thickness measurements of formed oxide layers,
- chemical composition analysis of deposits/oxides using a Jeol JSM-6610LV scanning electron microscope (SEM) working with an Oxford EDS (Energy Dispersive Spectroscopy),
- X-ray (XRD) measurements; the layer was subject to measurements using a Seifert 3003T/T X-ray diffractometer and the radiation originating from a tube with a cobalt anode ( $\lambda_{\text{Co}} = 0.17902\text{ nm}$ ). XRD measurements were performed in the  $20\div 120^{\circ}$  and  $5\div 120^{\circ}$  range. To interpret the results of the diffractograms were described by a Pseudo Voigt curve using the Analyze software. A computer software and the DHN PDS, PDF4+2009 crystallographic database were used for the phase identification,
- the oxide layer surfaces were studied using an Veeco atomic force microscope.

\* CZESTOCHOWA UNIVERSITY OF TECHNOLOGY, THE FACULTY OF PRODUCTION ENGINEERING AND MATERIALS TECHNOLOGY, 19 ARMII KRAJOWEJ AV., 42-200 CZESTOCHOWA, POLAND

# Corresponding author: gwozdzik@wip.pcz.pl

### 3. Results of examinations

After a long-term operation ( $T = 545^{\circ}\text{C}$ ,  $t = 200,000\text{h}$ ) 10CrMo9-10 steel shows degradation of bainitic-ferritic structure. The extent of degradation on the fire side is much higher than on the counter-fire side, which is presented in Fig. 1. A substantial depletion of boundary areas in carbide precipitates is visible on the fire side. Instead, in both cases carbide precipitates create ‘chains’ along boundaries, in certain places there are also cases of etching around sulphide precipitates and sporadic creep micropores on the

fire side. Corrosion on the grain boundaries also exists, both on the fire and counter-fire side, which is presented in Fig. 2. Such corrosion together with crevice corrosion to the largest extent occurs at the outside wall on the fire side, reaching  $84\ \mu\text{m}$  in depth. While on the counter-fire side at the outside wall corrosion exists on the grain boundaries to the depth of  $43\ \mu\text{m}$ . At the inside wall, on the fire and counter-fire side, corrosion on the grain boundaries exists to the depth of  $21\ \mu\text{m}$  and  $17\ \mu\text{m}$ , respectively.

Fig. 3 presents results of surface microscopic studies, where a greater degradation on the outside of tube wall is visible.

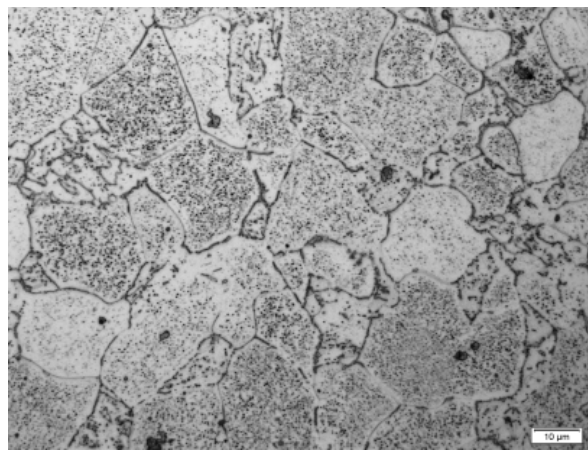
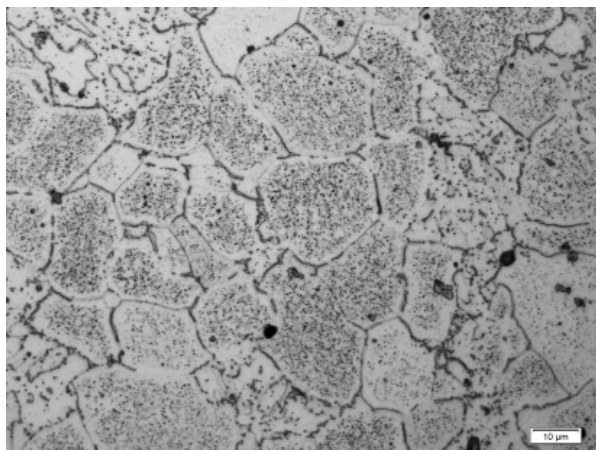


Fig. 1. Microstructure of 10CrMo9-10 steel operated for 200,000 hours at the temperature of  $545^{\circ}\text{C}$ , LM: (a) fire wall, (b) opposite fire wall

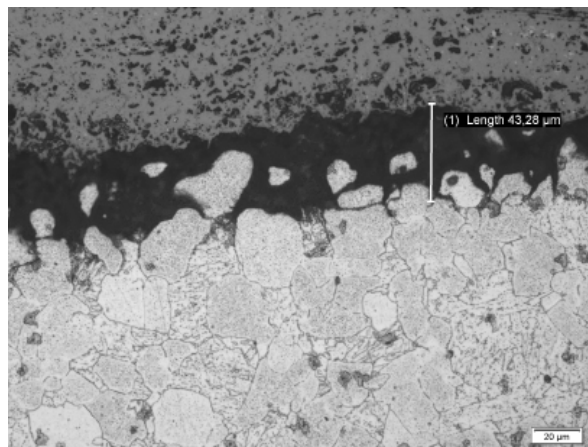
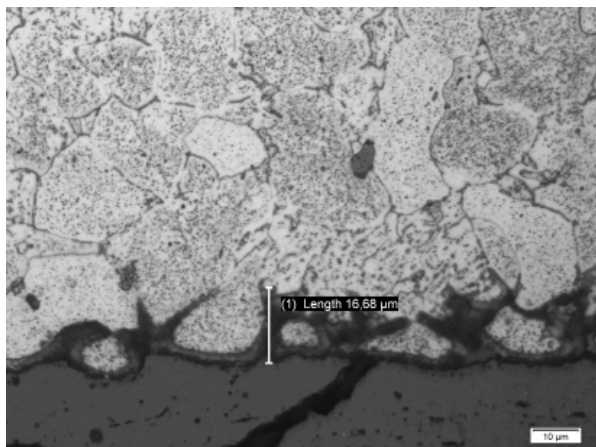
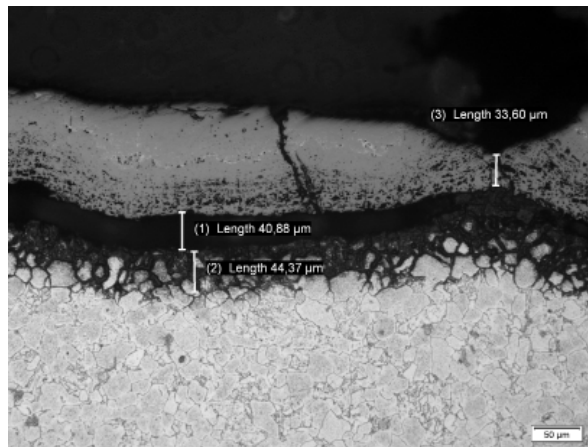
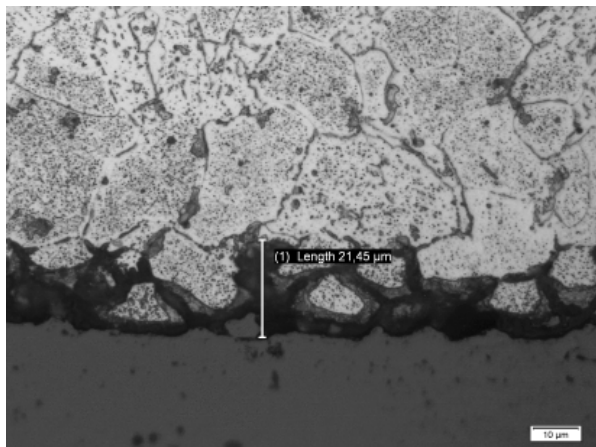


Fig. 2. Corrosion on the grain boundaries at: (a) inner surface – fire wall, (b) outer surface – fire wall, (c) inner surface – opposite fire wall, (d) outer surface – opposite fire wall



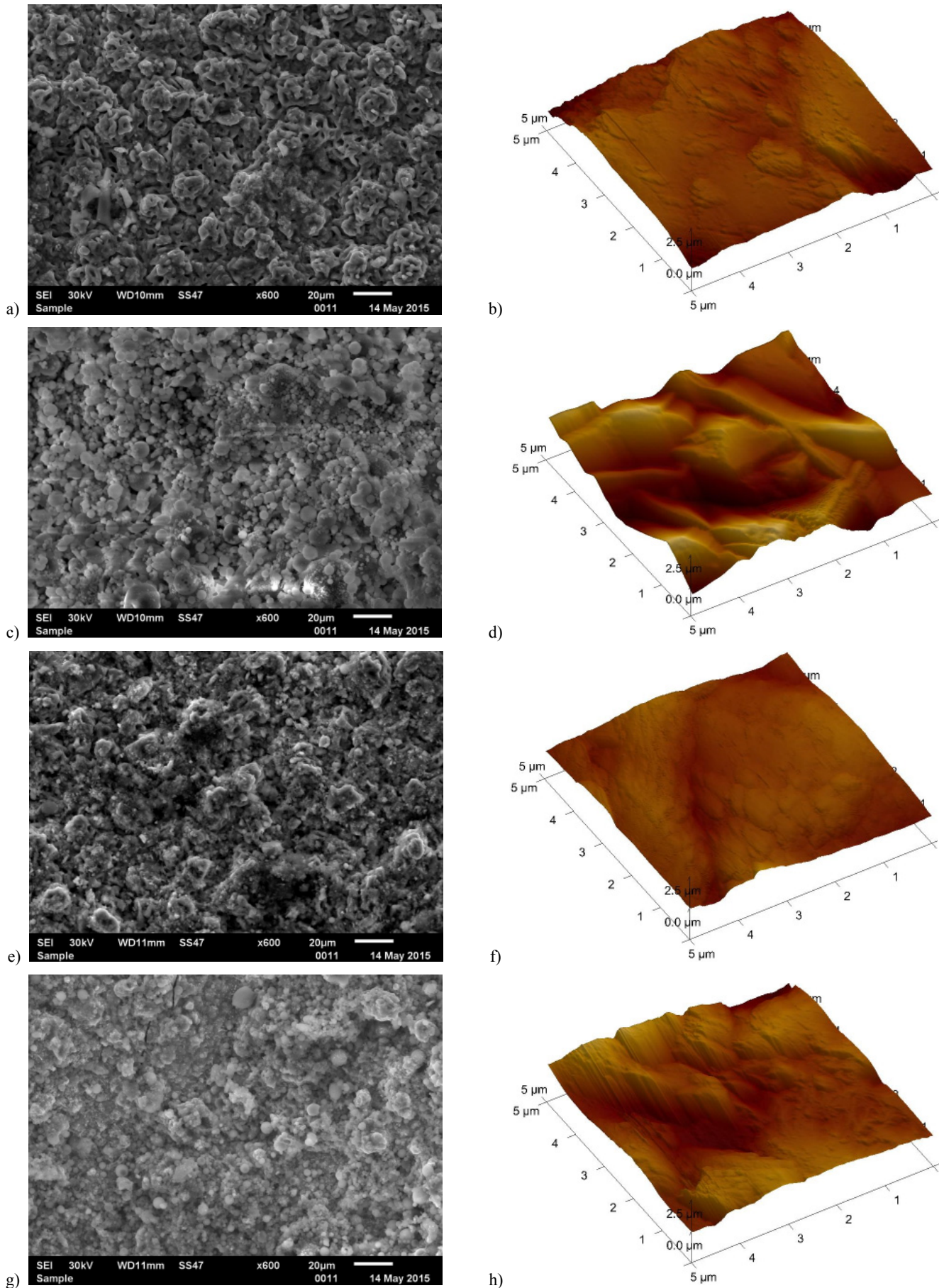


Fig. 3. Oxides formed on 10CrMo9-10 steel operated at 545°C during 200,000 hours: (a) inner surface – fire wall, SEM; (b) inner surface – fire wall, AFM; (c) outer surface – fire wall, SEM; (d) outer surface – fire wall, AFM; (e) inner surface – opposite fire wall, SEM; (f) inner surface – opposite fire wall, AFM; (g) outer surface – opposite fire wall, SEM; (h) outer surface – opposite fire wall, AFM

Fig. 3d and h shows spalling of individual deposit/oxide layers on the outside. In the case of fire side, both on the inside and outside, a larger degree of surface development was observed (Fig. 3a and c).

The surface topography studies (Figs. b, d, f, h and Table 1) have shown that the largest degree of surface development occurred on the outside surface on the fire side, where  $R_a$  and  $R_{max}$  were 406 nm and 2790 nm, respectively.

TABLE 1

Stereometric parameters

|   | Inner surface fire wall | Outer surface fire wall | Inner surface opposite fire wall | Outer surface opposite fire wall |
|---|-------------------------|-------------------------|----------------------------------|----------------------------------|
| Roughness average ( $R_a$ ), nm           | 157                     | 406                     | 146                              | 275                              |
| Maximum roughness depth ( $R_{max}$ ), nm | 1582                    | 2790                    | 1254                             | 2139                             |

The oxides layer thickness together with deposits on the fire side was 435  $\mu\text{m}$  and 820  $\mu\text{m}$  on the flowing medium and

flue gas side, respectively (Fig. 4a, b). For the counter-fire side on the inside the oxides layer thickness is smaller by 30  $\mu\text{m}$ , while on the outside by as many as 460  $\mu\text{m}$  (Fig. 4c, d). The layer formed on the fire outside shows high degradation, which is presented in Fig. 5b, where a surface after spalling of a thick deposit layer is visible. In addition, a very large fissure reaching the depth of 235  $\mu\text{m}$  may be noticed. Instead, on the inside only local spalling in the oxides layer may be observed directly on the flowing medium side (Fig. 5a).

Performed EDS analysis of chemical composition (Fig. 6) combined with X-ray phase analysis (Fig. 7) has shown that oxides occur on the inside surface of tube. Based on DHN PDS and PDF4+2009 crystallographic database it has been found that the forming oxides are:  $\text{Fe}_2\text{O}_3$  and  $\text{Fe}_3\text{O}_4$  in accordance with the catalogue card numbers: 01-079-0007, 01-089-0951, respectively. In the case of the outside surface of tube from opposite fire wall apart from the aforementioned compounds also Al, Si, K, Ca, Ti, Mg, Na and S based compounds exist, such as:  $\text{Al}_2\text{SiO}_5$ . The other elements, such as K, Ca, Ti, Mg, Na, occur in small amounts. Instead, directly on the fire outside only  $\text{Al}_2\text{SiO}_5$  exists and small amounts of K, P, S, Ca, Ti, Mg and Fe. After removing the external deposit layer on the outside and repeating the XRD analysis it has been shown that the forming oxide layer is built of  $\text{Fe}_2\text{O}_3$  and  $\text{Fe}_3\text{O}_4$  (Fig. 8).

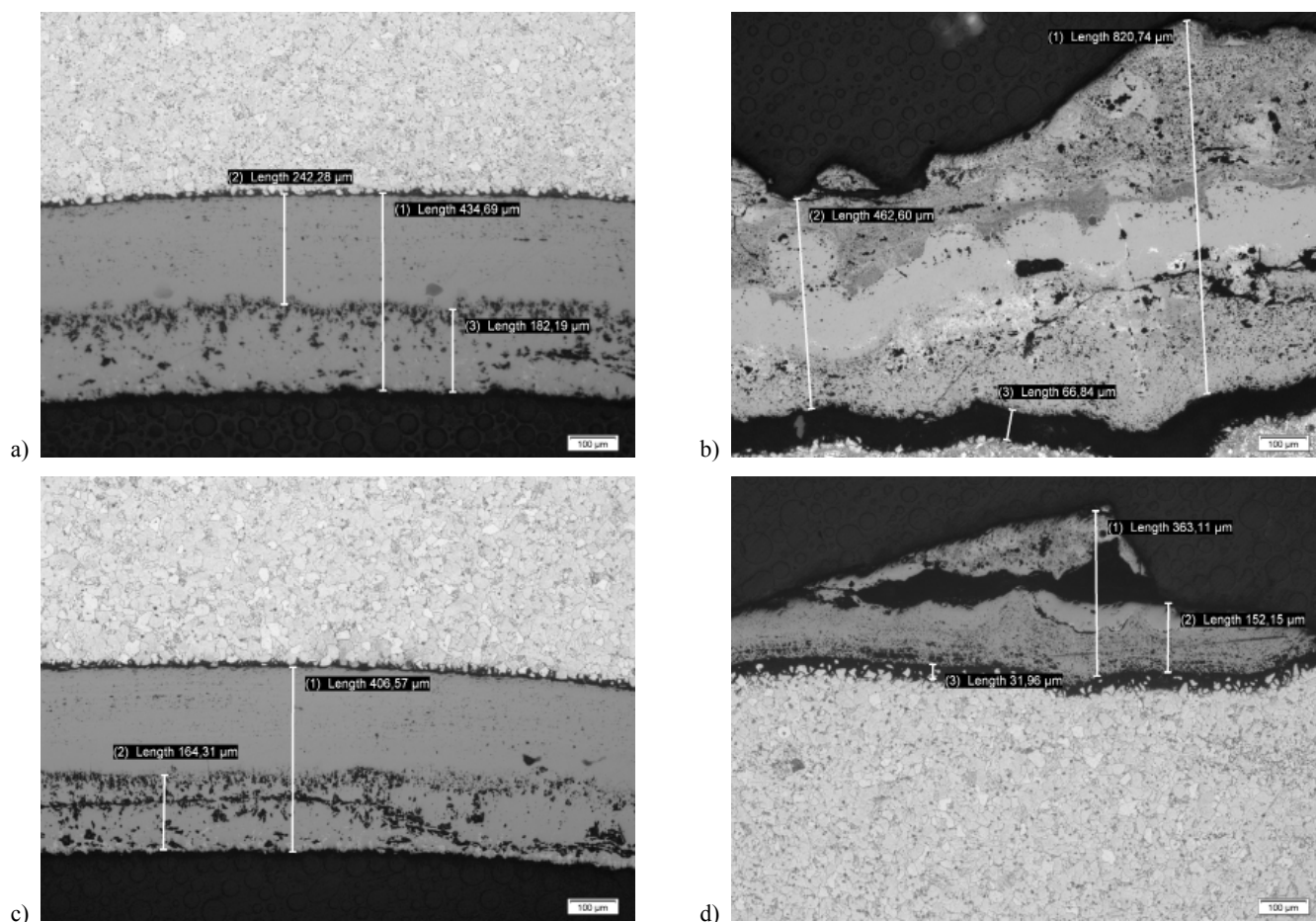


Fig. 4. The thickness of oxides layer formed on the steel examined, LM: (a) inner surface – fire wall, (b) outer surface – fire wall, (c) inner surface – opposite fire wall, (d) outer surface – opposite fire wall



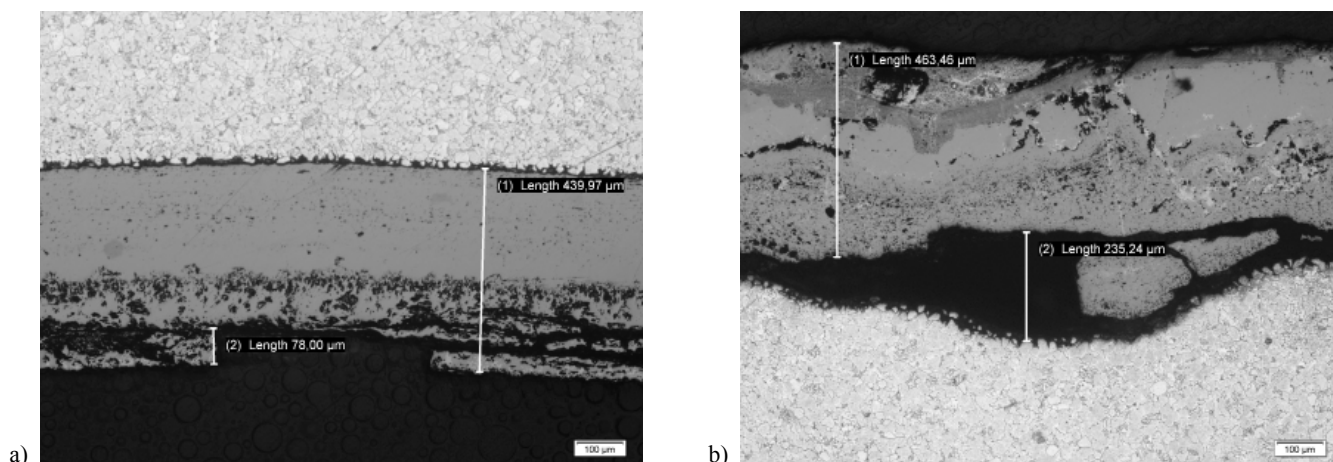


Fig. 5. The damage of oxide layer; cross section: (a) inner surface – fire wall, (b) outer surface – fire wall

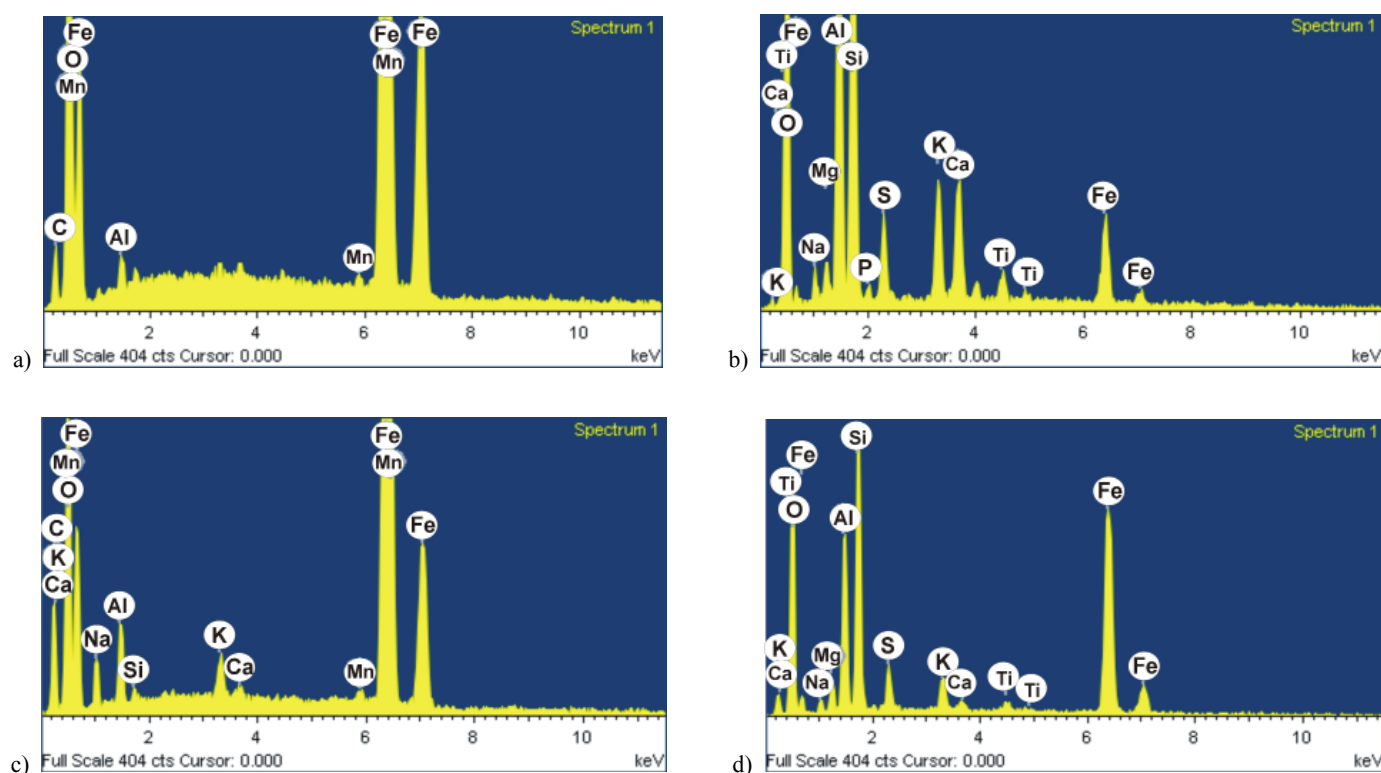


Fig. 6. EDS point microanalysis: (a) inner surface – fire wall, (b) outer surface – fire wall, (c) inner surface – opposite fire wall, (d) outer surface – opposite fire wall

#### 4. Summary

The oxide layer formed on 10CrMo9-10 steel after a long-term operation at an elevated temperature was examined. The oxide layer was studied on the fire and counter-fire side, formed both on the tube wall outside and inside. The obtained results have shown that the oxide layer formed on the fire side is more degraded. Apart from  $\text{Fe}_2\text{O}_3$  and  $\text{Fe}_3\text{O}_4$  oxides on the outside tube wall there are also deposits directly on the flue gas inflow side in the form of  $\text{Al}_2\text{SiO}_5$  reaching the depth of 400  $\mu\text{m}$  (fire side). The deposits/oxides layer on this side is more fissile, which was shown by microscopic studies and confirmed by surface

topography studies. On the flowing medium side (tube wall inside) there are places of spalling on the fire side, which have not been observed on the counter-fire side. Surface topography examinations have shown that  $R_a$  and  $R_{max}$  for the fire side were 157 nm and 1582 nm, respectively, while for the counter-fire side they were by 9 ( $R_a$ ) and 328 ( $R_{max}$ ) units lower.

In paper [2] (steel X10CrMoVNb9-1,  $T = 595^\circ\text{C}$ ,  $t = 54,144$  h) directly on the flue gas side consists of deposits based on Na, Al, Si, Ca, Ti, mainly sulphates, which occur both on the counter-fire and fire side.  $\text{MgSO}_4$  and  $\text{Mg}_2\text{Al}_4\text{Si}_5\text{O}_{18}$  occur additionally on the counter-fire side. Iron oxides such as  $\text{Fe}_2\text{O}_3$ ,  $\text{Fe}_3\text{O}_4$  and chromite  $\text{FeCr}_2\text{O}_4$  occur under deposits. The oxide layer is much

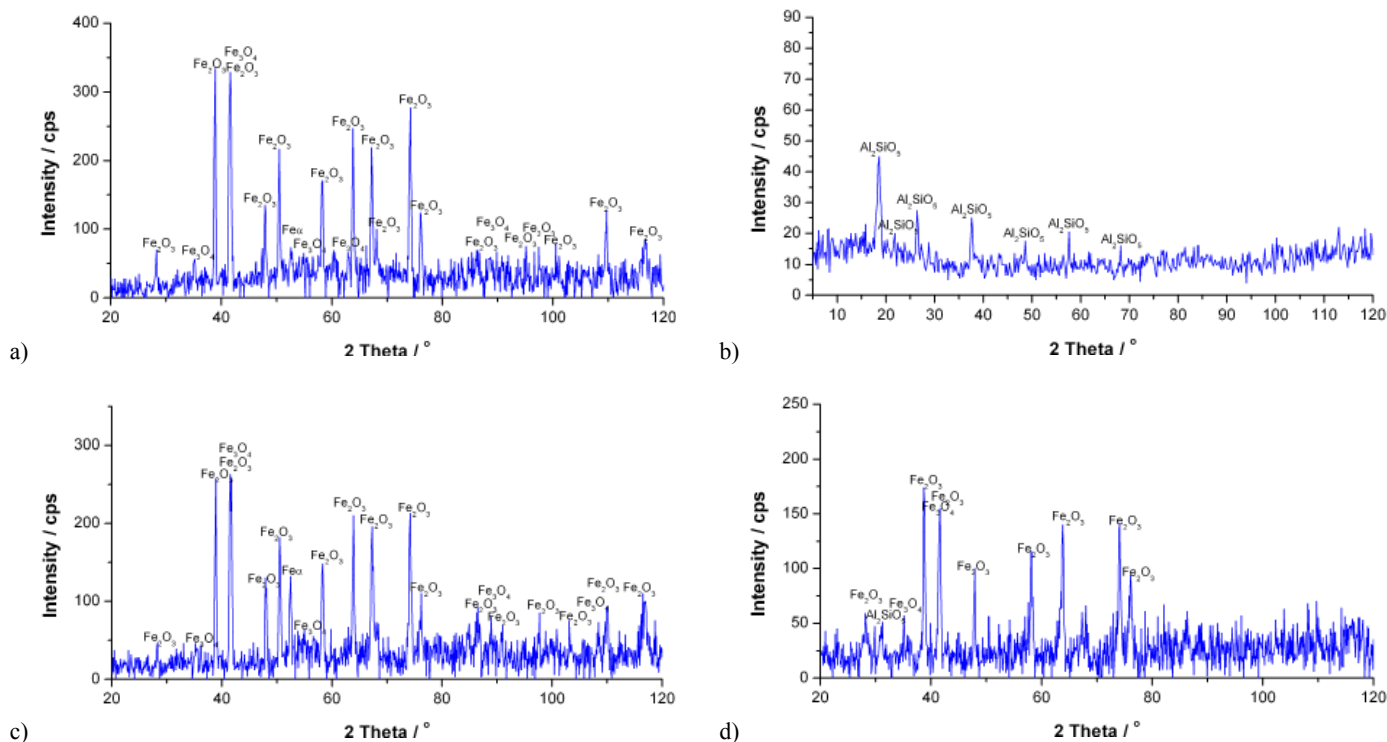


Fig. 7. Diffraction pattern of oxide layers obtained using the XRD technique: (a) inner surface – fire wall, (b) outer surface – fire wall, (c) inner surface – opposite fire wall, (d) outer surface – opposite fire wall

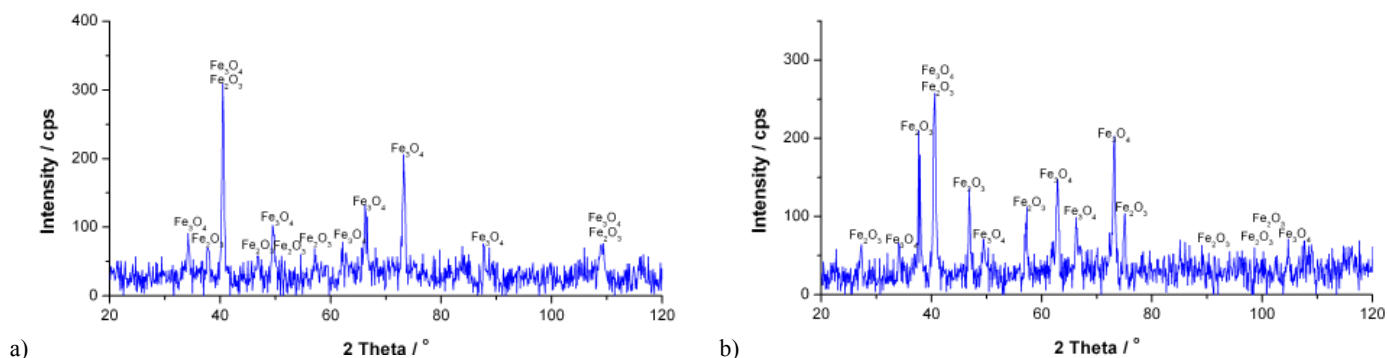


Fig. 8. Diffraction pattern of oxide layers after polishing obtained using the XRD technique: (a) outer surface – fire wall, (b) outer surface – opposite fire wall

more developed on the fire side and the oxide layer formed on the X10CrMoVNb9-1 steel on the fire side is the thicker than on the counter-fire side. A significant layer thickness on the fire side is caused by the formation of a larger amount of deposits.

#### REFERENCES

- [1] M. Gwoździk, Z. Nitkiewicz, Archives of Metallurgy and Materials **1**(58), 31 (2013).
- [2] M. Gwoździk, Z. Nitkiewicz, Archives of Civil and Mechanical Engineering **14**, 335 (2014).
- [3] J. Lehmusto, P. Yrjas, B.-J. Skrifvars, M. Hupa, Fuel Processing Technology **104**, 253 (2012).
- [4] B.-J. Skrifvars, R. Backman, M. Hupa, K. Salmenoja, E. Vakkilainen, Corrosion Science **50**, 1274 (2008).
- [5] R.K. Singh Raman, B.C. Muddle, International Journal of Pressure Vessels and Piping **79**, 585 (2002).
- [6] R.K. Singh Raman, Metallurgical and Materials Transactions A **29A**, 577 (1998).
- [7] J. Purbolaksono, A. Khinani, A.Z. Rashid, A.A. Ali, N.F. Nordin, Corrosion Science **51**, 1022 (2009).
- [8] F. Klepacki, D. Wywrot, XII Sympozjum Informacyjno-Szkoleniowe – Diagnostyka i remonty urządzeń ciepłno-mechanicznych elektrowni. Modernizacja urządzeń energetycznych w celu przedłużenia ich eksploatacji powyżej 300.000 godzin, Wisła 2010, 29.